Atmospheric Environment 178 (2018) 31–40

Contents lists available at ScienceDirect

Atmospheric Environment

journal homepage: www.elsevier.com/locate/atmosenv

Seasonal atmospheric deposition and air–sea gas exchange of polycyclic aromatic hydrocarbons over the Yangtze River Estuary, East China Sea: Implications for source–sink processes

Yuqing Jiang[a], Tian Lin[b], Zilan Wu[a], Yuanyuan Li[a], Zhongxia Li[a], Zhigang Guo[a,*], Xiaohong Yao[c]

[a] Shanghai Key Laboratory of Atmospheric Particle Pollution and Prevention, Institute of Atmospheric Sciences, Department of Environmental Science and Engineering, Fudan University, Shanghai 200433, China
[b] State Key Laboratory of Environmental Geochemistry, Institute of Geochemistry, Chinese Academy of Sciences, Guiyang 550081, China
[c] College of Environmental Science & Engineering, Ocean University of China, Qingdao 266100, China

ARTICLE INFO

Keywords:
Air–sea gas exchange
Dry deposition
Wet deposition
PAHs
Source–sink process
Yangtze River Estuary

ABSTRACT

In this work, air samples and surface seawater samples covering four seasons from March 2014 to January 2015 were collected from a background receptor site in the YRE to explore the seasonal fluxes of air–sea gas exchange and dry and wet deposition of 15 polycyclic aromatic hydrocarbons (PAHs) and their source–sink processes at the air–sea interface. The average dry and wet deposition fluxes of 15 PAHs were estimated as 879 ± 1393 ng m^{-2} d^{-1} and 755 ± 545 ng m^{-2} d^{-1}, respectively. Gaseous PAH release from seawater to the atmosphere averaged 3114 ± 1999 ng m^{-2} d^{-1} in a year round. The air–sea gas exchange of PAHs was the dominant process at the air–sea interface in the YRE as the magnitude of volatilization flux of PAHs exceeded that of total dry and wet deposition. The gas PAH exchange flux was dominated by three-ring PAHs, with the highest value in summer and lowest in winter, indicating a marked seasonal variation owing to differences in Henry's law constants associated with temperature, as well as wind speed and gaseous-dissolved gradient among seasons. Based on the simplified mass balance estimation, a net 11 tons y^{-1} of PAHs (mainly three-ring PAHs) were volatilized from seawater to the atmosphere in a ~20,000 km^2 area in the YRE. Other than the year-round Yangtze River input and ocean ship emissions, the selective release of low-molecular-weight PAHs from bottom sediments in winter due to resuspension triggered by the East Asian winter monsoon is another potential source of PAHs. This work suggests that the source–sink processes of PAHs at the air–sea interface in the YRE play a crucial role in regional cycling of PAHs.

1. Introduction

Polycyclic aromatic hydrocarbons (PAHs), as ubiquitous semi-volatile organic pollutants (Brown et al., 1996; Li et al., 2009; Nizzetto et al., 2008), have a critical threat to the health of humans and ecosystems due to their toxic, carcinogenic and bio-accumulative effects in organisms (Cai et al., 2016; Cheng et al., 2013). Unlike some persistent organic pollutants (POPs), use of which is prohibited globally, ongoing release of PAHs from primary sources are typically well associated with anthropogenic activities, mainly including vehicle exhausts, coal and biomass combustion, and the emission of petroleum products (Kavouras et al., 2001; Park et al., 2001; Qin et al., 2013); therefore, the fate of PAHs is a matter of greater concern than other POPs (Nizzetto et al., 2008). China is a significant emitter of PAHs, releasing 25,300 tons of 16 PAHs (as identified by the United States Environmental Protection Agency, US EPA) in 2003 (Xu et al., 2006). Due to the rapid economic development and growth in energy consumption, the emission of PAHs in China shows an increasing trend (Guo et al., 2006; Hu et al., 2011).

The land-derived PAHs can be widely distributed into marine environments through several processes, inclusive of atmospheric deposition, gas exchange at the air–sea interface, riverine input and facility effluents (Arzayus et al., 2001; Cai et al., 2016; Tsapakis et al., 2006; Yunker et al., 2002). The marginal seas, prone to PAH inputs from the adjacent land could thus act as the sink of these outflowed PAHs (Baker and Eisenreich, 1990; Kim and Chae, 2016; Lin et al., 2011; Mulder et al., 2014). However, the bidirectional gas exchange of PAHs implies that PAHs can also be delivered to the atmosphere from the water column, provided that the dissolved PAHs are oversaturated as compared to upper atmospheric PAH burdens (Bamford et al., 1999; Chen et al., 2016; Gigliotti et al., 2002). The released PAHs from the

* Corresponding author.
E-mail address: guozgg@fudan.edu.cn (Z. Guo).

https://doi.org/10.1016/j.atmosenv.2018.01.031
Received 3 October 2017; Received in revised form 10 January 2018; Accepted 17 January 2018
Available online 28 January 2018
1352-2310/

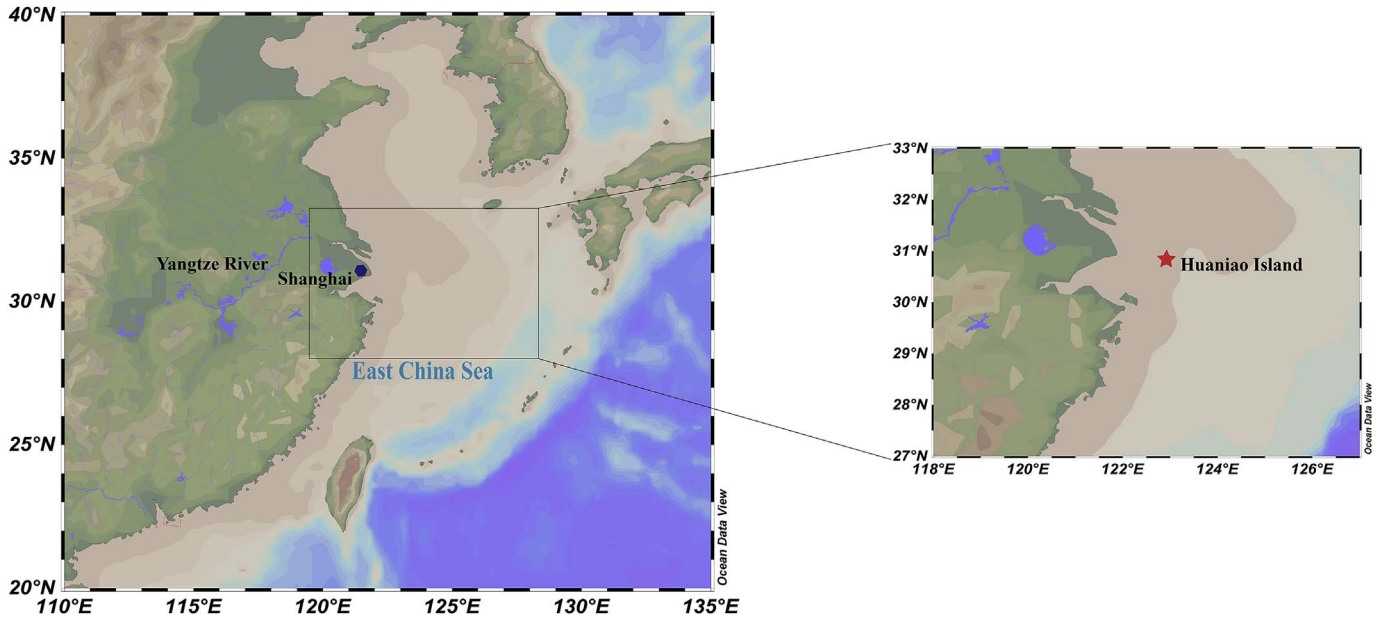

Fig. 1. Sampling site.

water column could then be atmospherically transported, and re-deposited in land areas (Fang et al., 2012). Therefore, a determination of the source–to–sink relationship of regional PAHs avails to reveal the biogeochemical cycling and dynamics of PAHs. However, the integrated air–sea gas exchange as well as dry and wet deposition of PAHs have been seldom touched in the East Asian marginal seas (Wu et al., 2017).

The Yangtze River Estuary (YRE), connected with the East China Sea (ECS) to the east (Fig. 1), is one of the world's largest and most prosperous estuaries, and is a home to over 15 million people (Feng et al., 2004). It accommodates more than 10% of the Chinese population and provides one-fifth of the national gross domestic product. The YRE is greatly influenced by the huge inputs from Yangtze River. As one of the largest rivers in the world, the Yangtze River drains an area of 1.94×10^6 km^2 and delivers 900 billion cubic meters of water, with 250 million tons of sediments and associated PAHs annually empting into the ECS through the YRE (Qi et al., 2014; Wang et al., 2007). Moreover, additional sources of PAHs in the marine environment of the ECS could be related to the long-range transport of continental air pollutants driven by the East Asian monsoon (Wang et al., 2014a; Zhang and Gao, 2007). It is reported that 8092 tons of PAHs are transported from mainland China to neighboring coastal areas annually, approximately 70% of which are retained within the offshore area (Lang et al., 2008). The ECS is greatly influenced by the Asian continental outflow under the westerly wind prevailing in winter and spring. As such, high levels of anthropogenic air pollutants or dust including PAHs from the Asian continent were transported across the ECS, with parts of which deposited to the ECS (Hsu et al., 2009). Conversely, the summer monsoon, which begins in late April, brings clean air masses originating from the west Pacific Ocean (Zhang et al., 2011). As one of the five main clusters in China, Yangtze River Delta port cluster in the YRE contains a large number of high-throughput ports. Concomitant with heavy marine traffic, high ship-based emissions generated could be a potentially local source of PAHs in the YRE and ECS. Recent surveys indicated that the PAH pollution in the YRE is more serious than that in other coastal areas of China. The concentrations of PAHs in YRE sediments were two-fold higher than those of the Yellow River Estuary (Hui et al., 2009). The total PAH concentrations in seawater of the ECS were higher than that in the South China Sea (Ren et al., 2010). Source analysis showed that the input from Yangtze River discharge was responsible for severe contamination in sediments, water and organisms in the YRE (Guo et al., 2007; Hung et al., 2014). Besides, the elevated concentrations of PAHs in seawater were due in part to the resuspension of sediments (Lin et al., 2013). PMF analysis showed that air–sea exchange represents 15.7% of the total atmospheric sources of particulate PAH over the ECS (Wang et al., 2014b). Most previous studies focused on the occurrence and concentrations of PAHs in the atmosphere, seawater, sediments, and zooplankton in the YRE and ECS on basis of cruise surveys, which usually processed within a few weeks. However, no study has estimated the seasonal air–sea gas exchange fluxes, as well as dry and wet deposition of PAHs in the YRE.

In this study, we collected 94 pairs of PAHs samples in ambient gas and aerosol phases at a receptor site Huaniao Island (HNI, 30.86°N, 122.67°E) in the YRE, covering four distinctive seasons when 20 surface seawater samples were also collected evenly. The objectives of the present study were to (1) estimate the seasonal dry and wet deposition fluxes and air–sea gas exchange flux of PAHs, (2) quantify the magnitude and direction of PAH exchange between air and sea compartments by integrating atmospheric deposition and air–sea gas exchange, and (3) establish the mass budget of PAHs at the air–sea interface in the YRE in a year round.

2. Materials and methods

2.1. Sampling site and sample collection

Ninety-four paired gas and particulate samples were collected at HNI in the YRE, ECS (Fig. 1). HNI is 66 km to the east of the Shanghai coast, and has an area of 3.28 km^2. It has fewer than 1000 inhabitants and no industrial activity. The sampling site was situated at the roof of a three-story building, at a height of about 50 m above the sea level. A sampler (Guangzhou Mingye Environmental Technology Company, Guangzhou, China) was used to collect ambient total suspended particulate (TSP) and gases simultaneously at a flow rate of 300 L/min for 23.5 h. The samples were collected evenly during four seasons: 27 March–18 April 2014 (spring, n = 23), 29 July–26 August 2014 (summer, n = 25), 16 October–10 November 2014 (autumn, n = 25) and 28 December 2014–18 January 2015 (winter, n = 21). The air mass first passed through a quartz filter (20 × 25 cm, 0.7 mm; Pall, Port Washington, NY) to gather particle-bound PAHs and then through a solvent-cleaned polyurethane foam (PUF) plug (length: 8.0 cm; diameter: 6.25 cm; density: 0.035 g cm^{-3}) to capture gaseous compounds. Prior to sampling, quartz filters were combusted at 450 °C for 4 h in a

muffle furnace and wrapped in aluminum foil until used. PUFs were cleaned by Soxhlet extraction for 48 h with acetone and dichloromethane (DCM).

A total of 20 surface seawater samples (ca. 25 L) and 11 rainwater samples were collected using a stainless steel bucket. The bucket was placed on the roof of the three-story building and opened only when it rained. Seawater samples were immediately filtered through pre-combusted glass fiber filters (GFFs) (Gelman Type A/E, Pall Gelman, USA; diameter: 150 mm; nominal pore size: 1 μm) to remove aerosol PAHs, and then dissolved phase PAHs was collected by XAD resin (Amberlite XAD-2 and XAD-4 mixture, Sigma-Aldrich, USA; 1:1 by volume) in a glass column (diameter: 25 mm, length: 200 mm). Samples were stored at −20 °C in a freezer until analysis.

2.2. Analysis of organics

PAHs were analyzed according to Mai et al. (2002) and Wang et al. (2014a). A mixture of deuterated compounds comprising acenaphthene (Ace-d_{10}, m/z = 164), phenanthrene (Phe-d_{10}, m/z = 188), chryene (Chr-d_{12}, m/z = 240), and perylene (Per-d_{12}, m/z = 264) was spiked into all samples as surrogate recovery to assess procedure performance prior to Soxhlet extraction. The air samples were Soxhlet extracted for 48 h in the laboratory using DCM. For the seawater and rainwater samples, XADs were ultrasonically extracted three times in a water bath with 100 mL DCM for 10 min. The extracts were then concentrated by a rotary evaporator and solvent-exchanged to n-hexane. The concentrated extracts were purified in a mixed chromatography column (diameter: 8 mm). The column was filled with 3 cm deactivated alumina, 3 cm deactivated silica gel, and 1 cm anhydrous sodium sulfate and eluted with 50 mL of a mixture of DCM and hexane (1:1 by volume). The extracts were concentrated to about 0.5 mL under a gentle stream of purified N_2. Hexamethylbenzene (HMB) was added as the internal standard to quantify PAHs before gas chromatography–mass spectrometry (GC–MS) analysis.

PAHs were measured by GC-MSD (Agilent GC 7890A coupled with 5975C MSD), using helium as the carrier gas. The oven temperature was first set at 60 °C for 2 min, then increased to 290 °C at 3 °C/min for 20 min. The post-run period lasted for 5 min with the temperature of 310 °C. The 15 PAHs measured were as follows: three-ring: acenaphthylene (Ac), acenaphthene (Ace), fluorene (Fl), phenanthrene (Phe), and anthracene (Ant); four-ring: fluoranthene (Flu), pyrene (Pyr), benzo[a]anthracene (BaA), and chrysene (Chr); five-ring: benzo[b]fluoranthene (BbF), benzo[k]fluoranthene (BkF), benzo[a]pyrene (BaP), and dibenzo[a,h]anthracene (DBA); six-ring: indeno[1,2,3-cd]pyrene (IP) and benzo[ghi]perylene (BghiP).

2.3. Quality assurance and quality control

Strict operational approaches were performed for quality control. Organic solvents used for extraction were of high-performance liquid chromatography grade. All of the vessels were cleaned using hot potassium dichromate-sulfuric acid lotion. The vessels were wrapped in aluminum foil, and baked at 450 °C for 4 h in a muffle furnace to remove contaminants. Vessels were rinsed three times with organic solvents before used. The method detection limits (MDLs) were calculated as the average field blank value plus three standard deviations. MDLs were 0.016–0.31 pg m^{-3} for air samples and 0.23–1.9 pg L^{-1} for water samples. Two field blanks for each season with a PAH level lower than the detection limit and three laboratory blanks lacking PAHs were analyzed using the same sample analysis approach as for samples. The breakthrough of the PUF samples was tested using two consecutive PUF plugs. The average surrogate recoveries of Ace-d_{10}, Phe-d_{10}, Chr-d_{12}, and Per-d_{12} were 71 ± 5%, 86 ± 10%, 100 ± 11% and 89 ± 15% for aerosol samples, respectively, and 79 ± 9%, 98 ± 10%, 90 ± 15% and 87 ± 13% for gaseous samples, respectively. The average recoveries of Ace-d_{10}, Phe-d_{10}, Chr-d_{12}, and Per-d_{12} were 80 ± 9%, 91 ± 11%, 92 ± 14% and 110 ± 10% for seawater samples, respectively, and 85 ± 9%, 88 ± 12%, 97 ± 14% and 107 ± 13% for rainwater samples, respectively.

2.4. Data treatment

Data treatment is described in Supplement S2.4, and includes flux estimation of air–sea gas exchange, dry and wet deposition and uncertainty estimation.

3. Results and discussion

3.1. Occurrence and source identification of PAHs in atmosphere

The sums of the atmospheric concentrations of the 15 PAHs during four seasons ranged from 1.2 to 16 ng m^{-3} (average: 4.4 ± 3.1 ng m^{-3}) in the gas phase, and from 0.21 to 30 ng m^{-3} (average: 3.4 ± 5.4 ng m^{-3}) in the aerosol phase, respectively. The concentrations of individual PAHs in the aerosols and gaseous phases during the four seasons are presented in Table S1. The concentrations of the 15 aerosol PAHs in this study were slightly lower than < 2.5-μm-diameter particulate matter ($PM_{2.5}$) concentrations of 16 PAHs (including naphthalene) at HNI from 2011 to 2012 (5.2 ± 5.8 ng m^{-3}) (Wang et al., 2014a). HNI could be considered as a background site for coastal ECS because of the long distance from land sources (66 km from the Shanghai shore). The total PAHs (gas and aerosol phases) can be regarded as much lower concentration levels relative to those reported at urban sites in China, *e.g.*, Shanghai (167 ng m^{-3}) (Chen et al., 2011), Beijing (223 ng m^{-3}) (Ma et al., 2011), and Guangzhou (130 ng m^{-3}) (Yang et al., 2010). Compared with the concentrations at the background site National Nature Reserve in the North China Plain (19 ng m^{-3}) (Zhu et al., 2014), the values at HNI were still evidently lower. The particulate concentrations of PAHs in this study were close to the value of 2.9 ng m^{-3} at a background site in Gosan, the South Korea, while the gaseous concentrations were higher than those of 1.4 ng m^{-3} in Gosan (Kim et al., 2012). Moreover, even lower concentrations of PAHs were observed at Eagle Harbor on Lake Superior (1000 pg m^{-3} for gases and 160 pg m^{-3} for particles) (Buehler et al., 2001) and the Noto peninsula in Japan (670 pg m^{-3} for particles) (Tang et al., 2015). Thus, the values of PAHs in this study may rank at the moderate level among those background sites.

In the aerosol phase, five- and six-ring PAHs predominated (average: 44%) among the 15 PAHs on an annual basis. Among 15 PAH compounds, high-molecular-weight BbF predominated, comprising 17% of the total aerosol-phase concentration, followed by Flu (14%), Pyr (11%), and Phe (11%). Three-ring PAH compounds accounted for 79% of the total in the gaseous phase, while five- and six -ring PAHs only comprised 1%. Ranked by percent contribution, the dominant congeners were Phe (51%), Fl (20%), and Flu (14%), which accounted for 85% of the total gaseous PAH concentrations in total.

The seasonal average atmospheric PAH concentrations in spring, summer, autumn, and winter were 1.8 ± 1.3 ng m^{-3}, 0.88 ± 0.32 ng m^{-3}, 1.3 ± 0.64 ng m^{-3}, and 11 ± 7.8 ng m^{-3} in the aerosol phase, respectively, and 3.5 ± 2.0 ng m^{-3}, 3.1 ± 0.95 ng m^{-3}, 3.4 ± 1.7 ng m^{-3}, and 7.9 ± 4.2 ng m^{-3} in the gaseous phase (Table S1). The highest atmospheric PAH concentrations in both phases were observed in winter (Fig. 2). Gas and aerosol phase concentrations of PAHs in the other three seasons were close and comparatively low. Northern China is an important PAH emission area, especially in winter, due to the longer winter season compared to the south, and heavy use of coal and firewood for heating (Xu et al., 2006). PAH levels were thus higher when air masses originating from northern China passed over HNI in winter, as illustrated by the three-day air-mass back trajectories in Fig. S1. A north-westerly wind blows towards the ocean from winter to spring, when HNI is exposed to PAH pollution from land by long-range transport. Increasing coal combustion and

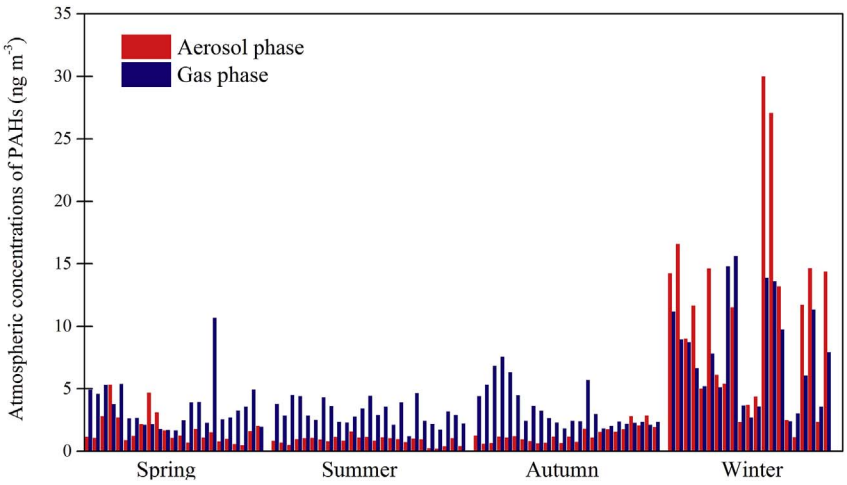

Fig. 2. Concentrations of gaseous and particulate polycyclic aromatic hydrocarbons (PAHs) in atmospheric samples in spring, summer, autumn, and winter collected in HNI, YRE.

biomass usage for heating in winter induces continental outflow, which has a high PAH burden (Guo et al., 2003, 2006; Wang et al., 2015; Wang et al., 2014a). The reduced atmospheric reactions resulting from the low ambient temperature and shorter period of daylight also contribute to the higher PAH concentrations in winter (Schifman and Boving, 2015).

Gaseous PAH levels tended to be low due to dilution by high-velocity wind. Wind speeds were negatively correlated with gaseous PAHs in winter ($R = -0.622$, $p < 0.01$, n = 21) (Fig. 3). Gaseous PAHs in winter were diffused and thus diluted by the influence of high-velocity wind. No such correlation was found in spring ($R = 0.045$, $p > 0.05$) or autumn ($R = -0.257$, $p > 0.05$). However, a positive correlation ($R = 0.567$, $p < 0.01$, n = 25) between wind speed and gaseous PAH concentration was found in summer, suggesting a possible local PAH source. High-velocity wind could induce substantial air–sea gas volatilization, resulting in elevated gaseous PAH concentrations in summer (Cheng et al., 2013). Thus, the increased gaseous PAHs emitted from local seawater in summer could offset the dilution effect of wind speed.

Diagnostic ratios are used to roughly identify the sources of PAHs (see Fig. 4). A value of Ant/(Ant + Phe) lower than 0.1 implies a petrogenic origin (Tobiszewski and Namiesnik, 2012). The average Ant/(Ant + Phe) ratio ranged from 0.06 ± 0.02 in spring to 0.10 ± 0.02 in autumn for aerosol phase PAHs, and from 0.02 ± 0.01 in spring to 0.08 ± 0.02 in autumn for gaseous PAHs, indicating a petroleum origin of PAHs in the atmosphere. BaA/(BaA + Chr) ratios lower than 0.2 indicate a petroleum source (Tobiszewski and Namiesnik, 2012). The mean value of this ratio was lower than 0.2 for gaseous PAHs in all four seasons, suggesting a petrogenic source. In the aerosol phase, the BaA/(BaA + Chr) ratio varied from 0.20 ± 0.09 in

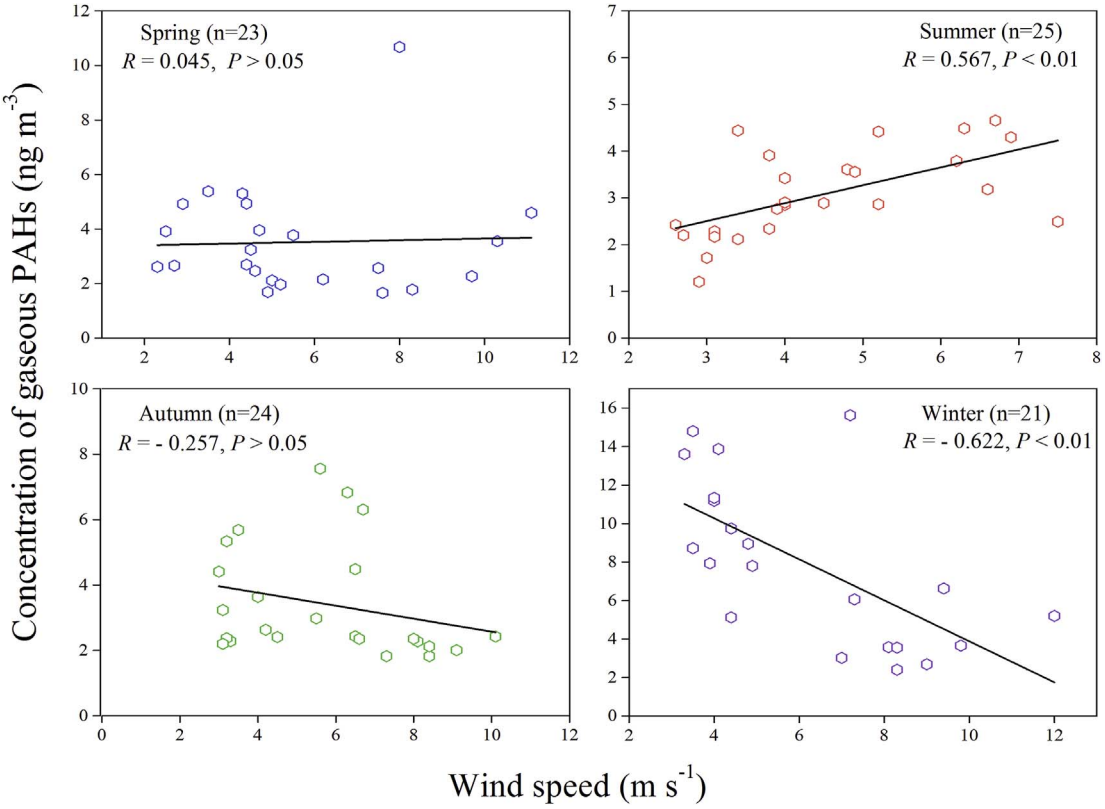

Fig. 3. Correlations of gaseous PAH concentrations and wind speed in spring, summer, autumn, and winter.

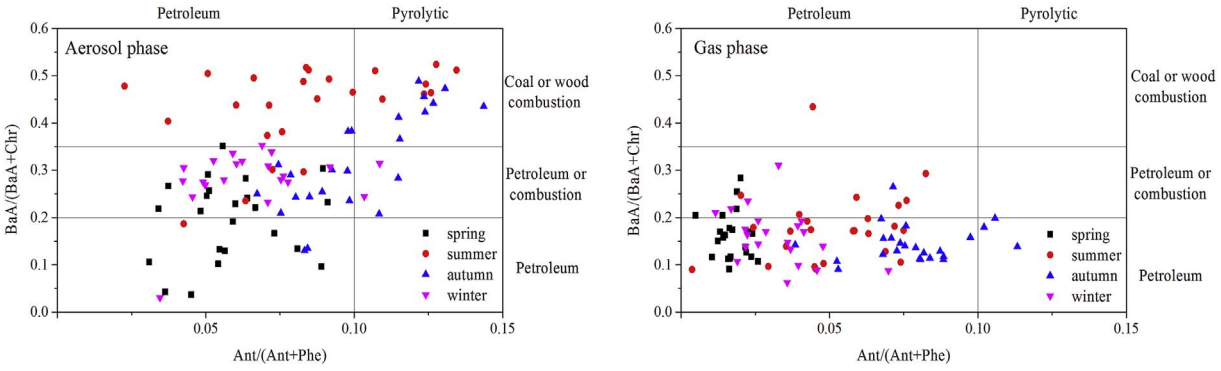

Fig. 4. Diagnostic ratios of PAHs in the aerosol and gaseous phases.

spring to 0.44 ± 0.09 in summer, indicating a petrogenic or combustion source. Therefore, the isomer ratios of PAHs indicated a mixture of petrogenic and pyrolytic sources for atmospheric PAHs over the YRE.

3.2. Occurrence of PAHs in seawater

The total concentrations of 15 dissolved PAHs in seawater ranged from 38.6 to 90.5 ng L^{-1}, with a mean of 61.4 ± 15.3 ng L^{-1}. The average concentrations of the 15 PAHs in seawater in spring, summer, autumn and winter were 63.7 ± 9.0 ng L^{-1}, 62.5 ± 22.7 ng L^{-1}, 48.8 ± 5.0 ng L^{-1} and 72.5 ± 6.0 ng L^{-1}, respectively. The dissolved concentrations of PAHs were slightly lower than those reported in a previous study in the ECS (20–31°N, 120–135°E, 70.2–120.3 ng L^{-1} for 10 PAHs) (Ren et al., 2010). The levels of dissolved PAHs were higher than those observed in the Mediterranean (13.1 ± 10.0 ng L^{-1} for 15 PAHs) (Guitart et al., 2007), south coastal area of Singapore (43.9 ± 35.8 ng L^{-1} for 16 PAHs) (He and Balasubramanian, 2010), and tropical coast of Taiwan (2.2 ± 1.2 ng L^{-1} for 22 PAHs) (Cheng et al., 2013). The levels of three-ring PAHs in seawater were high, and comprised 90% of the total PAH concentrations due to their high solubility and vapor pressure (Zhang et al., 2016). In this study, four-ring PAHs comprised 8% of the total dissolved PAHs, compared to 2% for five-six- ring PAHs, indicating a strong particle association for these high-molecular-weight PAHs. PAHs in seawater could originate from both pyrogenic and petrogenic sources, *e.g.,* incomplete fossil fuel combustion and accidental discharges of petroleum products from ships (Dachs et al., 1997). The high levels of three-ring PAHs in seawater in the YRE could be due to the Yangtze River input (Lin et al., 2013); and the oil pollution from ocean ships (Zhang et al., 2016). Ship-borne emissions are the highest in the coastal areas, and almost 70% occur within 400 km of land (Endresen et al., 2003; Fan et al., 2016). HNI is adjacent to the shipping routes in the ECS (less than 20 km to the main channel of the Yangtze River), under the impact of anthropogenic emissions transported from both Yangtze River Delta and Yangshan port. Yangshan port, which has a container-throughput capacity of more than 15 million TEU (Twenty-foot Equivalent Unit) is one of the largest ports in the world (Wang et al., 2016). Besides, HNI is located in the center of the ECS fishery zone; busy maritime traffic may be responsible for ship-related oil spills, and may be an important source of PAHs in this region.

3.3. Dry and wet deposition fluxes of PAHs

Dry deposition was estimated by assuming a deposition velocity of 0.3 cm/s during the sampling campaign (He and Balasubramanian, 2010; Ma et al., 2013). The annual dry deposition flux of particle-bound PAHs was 55 to 7771 ng m^{-2} d^{-1}, with a mean of 879 ± 1387 ng m^{-2} d^{-1} (Table S3). The average dry deposition flux in spring, summer, autumn and winter was 457 ± 324 ng m^{-2} d^{-1}, 228 ± 79 ng m^{-2} d^{-1}, 337 ± 166 ng m^{-2} d^{-1} and 2734 ± 2018 ng m^{-2} d^{-1}, respectively. As with the seasonal variation in aerosol-phase PAH concentrations, the highest value of dry deposition flux was in winter. The dry deposition flux of PAHs in this study was lower than that in urban areas, such as Butal, Turkey (7 μg m^{-2} d^{-1}) (Birgul et al., 2011), southern Taiwan (61 μg m^{-2} d^{-1}) (Sheu et al., 1996), and Chicago (144 μg m^{-2} d^{-1}) (Odabasi et al., 1999). These values were higher than those in rural and other coastal areas in western Greece (0.13 μg m^{-2} d^{-1}) (Terzi and Samara, 2005), Ulsan Bay, Korea (0.45 μg m^{-2} d^{-1}) (Lee and Lee, 2004), and southeastern Hong Kong Island (0.26 μg m^{-2} d^{-1}) (Liu et al., 2013).

The PAH concentration in rainwater samples was 55 to 1352 ng L^{-1} with a mean of 304 ± 362 ng L^{-1} during year-round sampling. The PAH composition of rainwater was dominated by three-ring PAHs (average: 90%), owing to their higher water solubility (Sahu et al., 2004). In comparison, four-ring and five- and six -ring PAHs comprised 7% and 3% of the total concentration, respectively. High-molecular-weight PAHs tended to partition to particles, while low-molecular-weight PAHs were commonly found in dissolved phase (Sahu et al., 2004). Consistent with previous reports (Olivella, 2006), the high proportion of low-molecular-weight PAHs indicates that dissolved PAHs had greater contribution to wet deposition than particle-associated PAHs in rainwater.

The wet deposition fluxes were 565 ± 317 ng m^{-2} d^{-1}, 1181 ± 606 ng m^{-2} d^{-1}, 477 ± 622 ng m^{-2} d^{-1} and 363 ng m^{-2} d^{-1} in spring, summer, autumn and winter, respectively, with an annual mean of 755 ± 545 ng m^{-2} d^{-1} (Table S4). The annual average wet deposition of PAHs was higher than those reported in the eastern Mediterranean Basin (291 ng m^{-2} d^{-1} for 13 PAHs) (Tsapakis et al., 2006), Galveston Bay (356 ng m^{-2} d^{-1} for 39 PAHs) (Park et al., 2001), and the southern Chesapeake Bay (87 ng m^{-2} d^{-1} for 14 PAHs) (Dickhut and Gustafson, 1995). In contrast, the values were lower than those in areas with intensive anthropogenic activities, such as Guangzhou, China (932 ng m^{-2} d^{-1} for 15 PAHs) (Guo et al., 2014), northern Italy (1 μg m^{-2} d^{-1} for 14 PAHs) (Olivella, 2006), and Butal (28 μg m^{-2} d^{-1} for 12 PAHs) (Birgul et al., 2011). A high frequency of rain (336.5 mm) was observed in summer, which was two-fold higher than that on an annual basis (157.6 mm). This likely explains the highest average wet deposition flux in summer. Despite having the highest PAH concentration in rainwater, precipitation was lowest in autumn (40.7 mm), which explains the low wet deposition flux of PAHs in this season. The lowest wet deposition flux occurred in winter, likely due to the low intensity of precipitation.

3.4. Air–sea gas exchange of PAHs

The air–sea gas exchange fluxes of PAHs were estimated using a two-film layer model (Supplement, S2.4). The uncertainties of air–sea gaseous exchange fluxes include systematic and random errors. Random errors in air–sea gaseous exchange flux were evaluated by

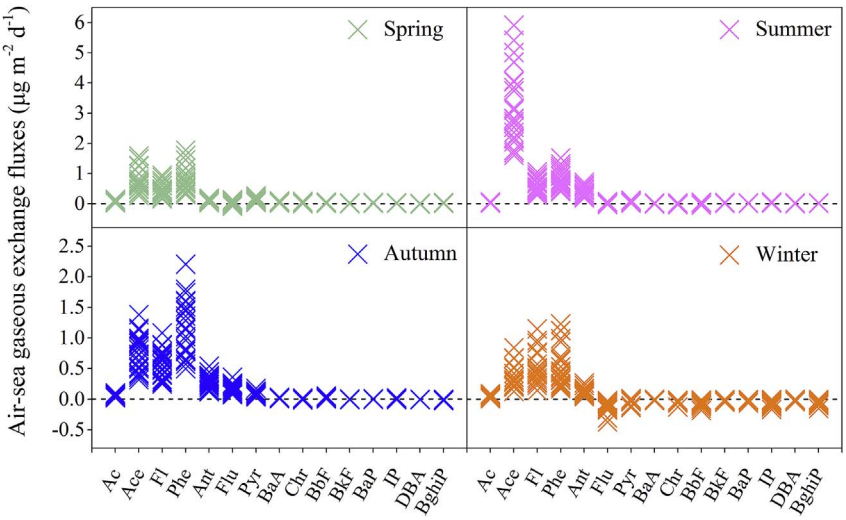

Fig. 5. Air–sea gas exchange fluxes of individual PAHs in spring, summer, autumn, and winter.

propagating the errors in mass transfer coefficient, concentrations of gaseous and dissolved PAHs and Henry's law constant (He and Balasubramanian, 2010; Nelson et al., 1998; Parnis et al., 2015). The uncertainty can be calculated by the equation:

$$\sigma^2(F) = \left(\frac{\delta F}{\delta k_{ol}}\right)^2 (\delta k_{ol})^2 + \left(\frac{\delta F}{\delta C_w}\right)^2 (\delta C_w)^2 + \left(\frac{\delta F}{\delta C_a}\right)^2 (\delta C_a)^2 + \left(\frac{\delta F}{\delta H}\right)^2 (\delta H)^2 \quad (1)$$

δH is assumed to be zero because H is a constant. The deviations are systematic errors. The uncertainty in k_{ol} is assumed to be 40%, as determined by random errors in mass transfer coefficients through layers of seawater and air (k_a and k_w) in previous studies (Nelson et al., 1998). The estimated error of gaseous and dissolved PAHs is ± 10%, based on the average standard deviation of surrogate recoveries. Considering above errors, the overall uncertainties of the air–sea gaseous exchange fluxes of PAHs ranged between 45% and 201%, with an average value of 95%.

The air–sea gas exchange fluxes of PAHs ranged from 308 ng m^{-2} d^{-1} to 9693 ng m^{-2} d^{-1} in all samples, with an average of 3114 ± 1999 ng m^{-2} d^{-1}. The positive value of air–sea gas exchange for the 15 PAHs during the whole sampling period (Fig. 5) indicated that the volatilization from surface seawater to the atmosphere was the governing process for PAHs in the YRE area, especially the low-molecular-weight PAHs. This suggests that YRE effluents are an important source of PAHs in the ambient atmosphere due to the intensive input of PAHs from the Yangtze River into the seawater in the YRE. The average volatilization value of PAHs was higher than those reported in the Raritan Bay (Gigliotti et al., 2002), Bohai Sea and Yellow Sea (Chen et al., 2016), and Atlantic Ocean (Nizzetto et al., 2008) due to the comparatively high concentration gradient at the interface. Volatilization tends to be higher in coastal areas due to the higher air–seawater concentration gradient caused by coastal sources of pollution, such as wastewater runoff (Chen et al., 2016). Lohmann et al. (2011) reported that the net volatilization of most PAHs in the Narragasett Bay occurred in the vicinity of the coastal area, while adsorption of PAHs occurred in the further area of the bay. Chen et al. (2016) reported that the net volatilization fluxes of low molecular weight PAHs decreased with distance from the coast in the Bohai Sea and Yellow Sea. Castro-Jiménez et al. (2012) showed that the samples collected near Alexandria and the Nile delta had the highest volatilization of PAHs in the southeast Mediterranean. Therefore, contaminated Yangtze River discharge could result in higher volatilization year-round in the YRE area.

The average net PAH volatilization fluxes were 2518 ± 1198 ng m^{-2} d^{-1}, 5215 ± 1956 ng m^{-2} d^{-1}, 3174 ± 1204 ng m^{-2} d^{-1} and 1196 ± 861 ng m^{-2} d^{-1} in spring, summer, autumn and winter, respectively. This indicates marked seasonal variation: PAH volatilization fluxes were highest in summer and lowest in winter. Spring and autumn exhibited moderate PAH volatilization fluxes.

The seasonal flux variation of PAHs could be caused by Henry's law constants and gaseous-dissolved gradient differences among seasons. Henry's law constants are strongly associated with the water temperature. The constants enlarge about 10-fold with an increase temperature of 25 °C (Nelson et al., 1998). Air–sea gas exchange fluxes exhibited positive associations with temperature (Gevao et al., 1998). A higher temperature results in higher PAH volatilization fluxes (Cheng et al., 2013; Gevao et al., 1998). The flux of PAHs was a marked function of seawater temperature in our study. PAH flux was positively correlated with temperature in all four seasons ($R^2 = 0.59$, $p < 0.05$, n = 94) (Fig. S3). Higher values of Henry's law constants due to high temperature in summer could explain the elevated air–sea gas exchange fluxes in this season. The PAH gaseous-dissolved gradient is the other factor influencing the PAH fluxes. Greater PAH gaseous-dissolved gradient results in the higher air–sea gas exchange fluxes. The volatilization flux of PAHs was highest in summer because the lowest PAH concentrations in the gaseous phase were in this season due to the easterly clean air mass brought by East Asian monsoon from the ocean (Wang et al., 2014a). Moreover, dissolved PAH loads from the Yangtze River in wet season, especially summer, are higher than that in dry season (Qi et al., 2014). The strong erosion process can transport the residual PAHs from soils to the water column in the wet season. Lowest concentrations of atmospheric PAHs and relatively high concentrations of dissolved PAHs in summer thus increased the PAH gaseous-dissolved concentration gradient.

Four typical PAHs with different numbers of rings were used to delineate the yearly variation of gaseous exchange at the air–sea interface (Fig. 6). Ace (three rings) exhibited the highest volatilized air–sea gas flux among the 15 PAHs. Similar results were reported in the Lake Chaohu, China (Qin et al., 2013) and the Patapsco River, Chesapeake Bay, United States (Bamford et al., 1999). This is likely due to its high volatility and lower K_{ow} (Vardar et al., 2008). The volatilization flux of Ace in summer was extremely high, with a value of 3216 ± 1216 ng m^{-2} d^{-1}. Lower volatilization was detected in spring (746 ± 364 m^{-2} d^{-1}), autumn (751 ± 283 ng m^{-2} d^{-1}), and winter (360 ± 185 ng m^{-2} d^{-1}), respectively. This was driven by the higher temperature and higher Ace concentrations in surface seawater, resulting in a higher air–sea concentration gradient. The gaseous-phase Ace concentration was lowest in summer due to the clean air mass brought by the summer monsoon; in the dissolved phase, Ace was the most abundant PAH (59%) in summer. Ace originates from incomplete

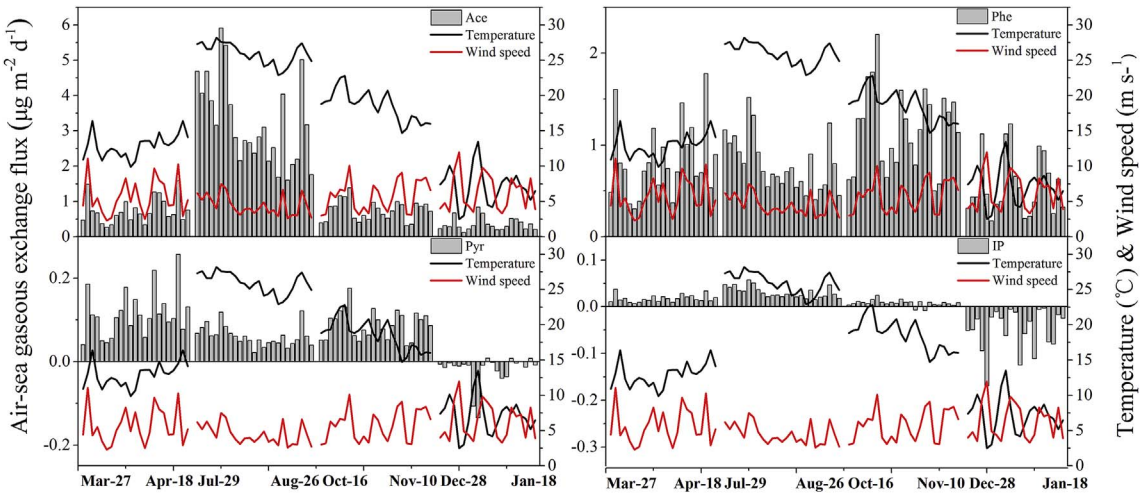

Fig. 6. Air–sea gas exchange fluxes of acenaphthene (Ace), phenanthrene (Phe), pyrene (Pyr), and indeno[1,2,3-cd] pyrene (IP) in spring, summer, autumn, and winter.

combustion sources, such as industrial production (Reisen and Arey, 2002). The Yangtze River input is greatest in the wet season, which may transport more Ace from the land into the sea (Qi et al., 2014).

Phe (three rings) was also highly volatilized year-round but showed no pronounced seasonal variation, (average: 825 ± 398 ng m^{-2} d^{-1}, 796 ± 296 ng m^{-2} d^{-1}, 1179 ± 448 ng m^{-2} d^{-1}, and 565 ± 331 ng m^{-2} d^{-1} in spring, summer, autumn and winter, respectively). In winter, the gaseous-phase PAH concentrations increased because of the contaminated long-range air mass transported from the mainland. The gaseous-phase Phe concentration in winter was two-fold those in the other three seasons. Nevertheless, unlike the deposition trend for the four-to six-PAHs, the Phe volatilization flux was similar to those in the other three seasons. This could be explained by the sustained source of dissolved Phe. The high wind velocity associated with the East Asian winter monsoon, results in release of large quantities of three-ring PAHs from sediments into seawater, particularly Phe in winter (Lin et al., 2013). Therefore, the increased Phe concentration in the dissolved phase could sustain the high volatilization of Phe in winter.

Low-molecular-weight PAHs tended to volatilize year-round, while high-molecular-weight PAHs tended to be deposited especially in winter. Due to long-range transport of contaminants from mainland China, the gaseous-phase high-molecular-weight PAH concentrations were highest in winter. Pyr (four rings) volatilized from spring to autumn (average: 88 ± 45 ng m^{-2} d^{-1}), and was deposited in winter (−19 ± 36 ng m^{-2} d^{-1}). IP (six rings) undergoes a slight volatilization from spring to autumn (average: 19 ± 13 ng m^{-2} d^{-1}), which was close to equilibrium. However, IP exhibited marked deposition in winter (−50 ± 45 ng m^{-2} d^{-1}).

Our findings suggest that the low-molecular-weight PAHs are volatilized year-round in the YRE. To our knowledge, this has not been reported previously. Some areas undergo gas deposition year-round, such as the eastern Mediterranean Basin (Tsapakis et al., 2006) and the coastal region of Incheon, South Korea (Kim and Chae, 2016). Other areas experience a deposition flux of PAHs in winter and volatilization flux in other seasons. In Wolftrap, southern Chesapeake Bay, PAH flux is from the water column in spring, summer, and autumn, but it is reversed in winter (Gustafson and Dickhut, 1997). In Esthwaite Water, UK, adsorption flux was observed in November, the coldest month (Gevao et al., 1998). Gaseous volatilization of PAHs in winter suggests additional sources in water-column sources, such as the release of three-ring PAHs from the YRE's sediments, which could sustain volatilization in winter in the YRE (Lin et al., 2013).

3.5. Implications for the source–sink processes of PAHs at the air–sea interface

The annual average values of PAH air–sea gas volatilization flux, dry deposition and wet deposition were 3114 ± 1999 ng m^{-2} d^{-1}, 879 ± 1393 ng m^{-2} d^{-1} and 755 ± 545 ng m^{-2} d^{-1}, respectively

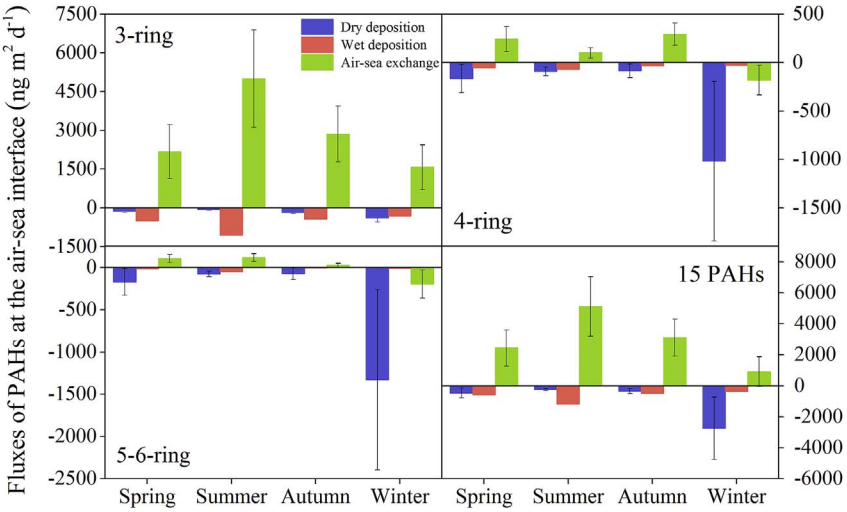

Fig. 7. Dry and wet deposition and air–sea gas exchange fluxes of PAHs.

(Fig. 7). The absolute PAH air–sea exchange flux values exceeded those of dry and wet deposition by factors of three and four, indicating that air–sea gas volatilization is the dominant process for PAH exchange at the air–sea interface. Based on the average gas exchange and deposition values in four seasons, the integrated net volatilization flux was 1441 ng m^{-2} d^{-1} at the air–sea interface in one year's sampling (Table S5). This suggests that the marine system could be a secondary source of PAHs to the atmosphere, and may play a key role in regional biogeochemical cycling of PAHs. Seasonally, absorptive integrated net fluxes of PAHs occurred only in winter (−1900 ng m^{-2} d^{-1}) due to the lower volatilization flux from seawater and increased dry deposition flux. The other three seasons showed a tendency towards PAH volatilization; average integrated net fluxes were 1496 ng m^{-2} d^{-1}, 3806 ng m^{-2} d^{-1}, and 2360 ng m^{-2} d^{-1} in spring, summer, and autumn, respectively.

Three-ring PAHs exhibited mainly volatilized air–sea gas exchange fluxes in all four seasons. The integrated net flux of the three-ring PAHs showed a tendency towards year-round due to much higher rate of evaporation from seawater, with the average ranging from 869 ng m^{-2} d^{-1} in winter to 3880 ng m^{-2} d^{-1} in summer. Seawater was hence the source of the three-ring PAHs in the YRE based on the annual integrated net flux. The integrated net flux of the four-ring PAHs was close to equilibrium in spring (24 ng m^{-2} d^{-1}) and summer (−61 ng m^{-2} d^{-1}), but showed slight volatilization in autumn (174 ng m^{-2} d^{-1}). In winter, dry deposition exceeded gas absorption flux by a factor of nearly 3, inducing a significant deposition process of PAHs (−1231 ng m^{-2} d^{-1}) between the atmosphere and seawater compartments. The high deposition fluxes in winter suggest that the seawater acts as a sink for the four-ring PAHs in one year. The direction of the integrated net flux for the five-to six -ring PAHs was from the atmosphere to seawater in all four seasons, with the average value ranging from −13 ng m^{-2} d^{-1} in summer to −1538 ng m^{-2} d^{-1} in winter. This showed that the seawater was a sink for the five-to six-ring PAHs in all four seasons in the YRE. Deposition of the five-to six-ring PAHs was high in winter due to a greater deposition of dry particulates deposition and gas exchange. Therefore, the seawater was the sink for five-to six-ring PAHs in the YRE year-round.

A simplified mass balance was established to evaluate the PAH exchange status at the air–sea interface in the YRE (~20,000 km^2). The annual dry and wet deposition fluxes of PAHs for the YRE were 6.9 ± 10 tons y^{-1} and 4.7 ± 4.0 tons y^{-1}, respectively. The air–sea gas exchange flux from seawater to the atmosphere was estimated to be 23 ± 15 tons y^{-1}. As a result, 11 tons y^{-1} of PAHs was net volatilized from the seawater to the atmosphere for integrating air–sea gas exchange and deposition. The volatized flux was mainly three-ring PAHs (21 ± 13 tons y^{-1}), accounting for 90% of the total air–sea gas exchange flux. This is consistent with previous reports (Chen et al., 2016; Cheng et al., 2013), and suggests that the seawater acts as the secondary source of three-ring PAHs to the ambient atmosphere, while dissolved PAHs existing in the water column must receive other sources to sustain their volatilization tendency. In winter, East Asian monsoon-triggered atmospheric turbulence and ocean currents tended to desorb more particle-bound PAHs from the sediments to seawater by strong suspension (Cheng et al., 2013). 49 tons y^{-1} of PAHs is released to the seawater from the sediments in the YRE-inner shelf ECS (based on an area of 80,000 km^2), which are mostly three-ring Phe (Lin et al., 2013). In this work, the increased concentration of dissolved Phe in seawater in winter was likely due to the resuspension of sediments triggered by the East Asian winter monsoon. Therefore, the resuspension process of sediments in the water column could be an important source of dissolved PAHs in the seawater. Considering that three-ring PAHs are released from sediments in the coastal ECS (~80,000 km^2), it was estimated that the gas exchange flux of three-ring PAHs from seawater to the ambient atmosphere was 84 tons y^{-1} based on an area of 80,000 km^2, which was higher than that of the 49 tons y^{-1} released from bottom sediments. The volatilization flux of three-ring PAHs from water should be higher than 84 tons y^{-1}, due to the higher wind velocities in the open sea than in the YRE, and higher air-seawater concentration gradient attributed to the lower gaseous concentrations in the open sea. This implies that volatilization is a mechanism of removal of dissolved PAHs (mainly three-ring PAHs) in the water column in the coastal ECS when large quantities of PAHs are transported to the area by the Yangtze River. Together with the release from suspended particulates, petroleum emissions and leakage from ocean ships could also be sources of dissolved three-ring PAHs in seawater, as discussed above. These sources of PAHs may sustain the volatilization of three-ring PAHs from seawater to the atmosphere in the region, suggesting that the air–sea gas exchange fluxes of PAHs at the air–sea interface in the YRE play an important role in regional cycling of PAHs.

4. Conclusions

This study determined the seasonal concentration, composition and origin of particulate and gaseous PAHs in atmosphere and dissolved PAHs in seawater in the YRE. Volatilization of PAHs from seawater to the atmosphere exhibited marked seasonal variation. The three-ring PAHs showed a considerable net volatilization year-round, even in the presence of higher atmospheric concentrations in winter. Three-ring PAHs released from the resuspension and transport of bottom sediments driven by the winter East Asian monsoon could be an important PAH source of the water in winter, and may result in their volatilization. The four-ring PAHs showed a tendency towards volatilization from spring to autumn, but exhibited marked deposition in winter. The five-to six-ring PAHs showed high depositional fluxes in winter, but were in equilibrium in the other three seasons. The volatilization of the 15 PAHs from seawater (mainly sourced from the Yangtze River input and ocean ship oil contamination) was estimated to be 23 ± 15 tons y^{-1} (with an area of 20,000 km^2). The annual dry and wet deposition fluxes for the YRE were 6.9 ± 10 tons y^{-1} and 4.7 ± 4.0 tons y^{-1}, respectively. Overall, the seawater is a potential source for the PAHs in the upper atmosphere over the YRE based on the annual integrated net flux (11 tons y^{-1}). The combined sources of PAHs from the Yangtze River input, ship oil contamination and the released PAHs from the bottom sediments sustain the PAH volatilization from seawater in the region.

Acknowledgements

This work was financially supported by National Basic Research Program of China (2016YFA0601304, No: 2014CB953701) and the National Natural Science Foundation of China (NSFC) (Nos: 41376051, 41573134 and 41176085). The anonymous reviewers should be sincerely appreciated for their constructive comments that greatly improved this work.

Appendix A. Supplementary data

Supplementary data related to this article can be found at http://dx.doi.org/10.1016/j.atmosenv.2018.01.031.

References

Arzayus, K.M., Dickhut, R.M., Canuel, E.A., 2001. Fate of atmospherically deposited polycyclic aromatic hydrocarbons (PAHs) in Chesapeake Bay. Environ. Sci. Technol. 35, 2178–2183.

Baker, J.E., Eisenreich, S.J., 1990. Concentrations and fluxes of polycyclic aromatic-hydrocarbons and polychlorinated-biphenyls across the air-water-interface of lake-superior. Environ. Sci. Technol. 24, 342–352.

Bamford, H.A., Offenberg, J.H., Larsen, R.K., Ko, F.C., Baker, J.E., 1999. Diffusive exchange of polycyclic aromatic hydrocarbons across the air-water interface of the Patapsco River, an urbanized subestuary of the Chesapeake Bay. Environ. Sci. Technol. 33, 2138–2144.

Birgul, A., Tasdemir, Y., Cindoruk, S.S., 2011. Atmospheric wet and dry deposition of polycyclic aromatic hydrocarbons (PAHs) determined using a modified sampler. Atmos. Res. 101, 341–353.

Brown, J.R., Field, R.A., Goldstone, M.E., Lester, J.N., Perry, R., 1996. Polycyclic aromatic

hydrocarbons in central London air during 1991 and 1992. Sci. Total Environ. 177, 73–84.
Buehler, S.S., Basu, I., Hites, R.A., 2001. A comparison of PAH, PCB, and pesticide concentrations in air at two rural sites on Lake Superior. Environ. Sci. Technol. 35, 2417–2422.
Cai, M., Liu, M.Y., Hong, Q.Q., Lin, J., Huang, P., Hong, J.J., Wang, J., Zhao, W.L., Chen, M., Cai, M.H., Ye, J., 2016. Fate of polycyclic aromatic hydrocarbons in seawater from the Western Pacific to the Southern ocean (17.5 degrees N to 69.2 degrees S) and their inventories on the Antarctic shelf. Environ. Sci. Technol. 50, 9161–9168.
Castro-Jiménez, J., Berrojalbiz, N., Wollgast, J., Dachs, J., 2012. Polycyclic aromatic hydrocarbons (PAHs) in the Mediterranean Sea: Atmospheric occurrence, deposition and decoupling with settling fluxes in the water column. Environ. Pollut. 166, 40–47.
Chen, Y.J., Feng, Y.L., Xiong, S.C., Liu, D.Y., Wang, G., Sheng, G.Y., Fu, J.M., 2011. Polycyclic aromatic hydrocarbons in the atmosphere of Shanghai, China. Environ. Monit. Assess. 172, 235–247.
Chen, Y.J., Lin, T., Tang, J.H., Xie, Z.Y., Tian, C.G., Li, J., Zhang, G., 2016. Exchange of polycyclic aromatic hydrocarbons across the air-water interface in the Bohai and Yellow Seas. Atmos. Environ. 141, 153–160.
Cheng, J.O., Ko, F.C., Lee, C.L., Fang, M.D., 2013. Air-water exchange fluxes of polycyclic aromatic hydrocarbons in the tropical coast, Taiwan. Chemosphere 90, 2614–2622.
Dachs, J., Bayona, J.M., Raoux, C., Albaigés, J., 1997. Spatial, vertical distribution and budget of polycyclic aromatic hydrocarbons in the Western Mediterranean seawater. Environ. Sci. Technol. 31, 682–688.
Dickhut, R.M., Gustafson, K.E., 1995. Atmospheric input of selected polycyclic aromatic hydrocarbons and polychlorinated biphenyls to southern Chesapeake Bay. Mar. Pollut. Bull. 30, 385–396.
Endresen, O., Sorgard, E., Sundet, J.K., Dalsoren, S.B., Isaksen, I.S.A., Berglen, T.F., Gravir, G., 2003. Emission from international sea transportation and environmental impact. Journal of Geophysical Research-Atmospheres 108.
Fan, Q.Z., Zhang, Y., Ma, W.C., Ma, H.X., Feng, J.L., Yu, Q., Yang, X., Ng, S.K.W., Fu, Q.Y., Chen, L.M., 2016. Spatial and seasonal dynamics of ship emissions over the Yangtze River delta and East China Sea and their potential environmental influence. Environ. Sci. Technol. 50, 1322–1329.
Fang, M.-D., Lee, C.-L., Jiang, J.-J., Ko, F.-C., Baker, J.E., 2012. Diffusive exchange of PAHs across the air–water interface of the Kaohsiung Harbor lagoon, Taiwan. J. Environ. Manag. 179–187.
Feng, H., Han, X.F., Zhang, W.G., Yu, L.Z., 2004. A preliminary study of heavy metal contamination in Yangtze River intertidal zone due to urbanization. Mar. Pollut. Bull. 49, 910–915.
Gevao, B., Hamilton-Taylor, J., Jones, K.C., 1998. Polychlorinated biphenyl and polycyclic aromatic hydrocarbon deposition to and exchange at the air-water interface of Esthwaite water, a small lake in Cumbria, UK. Environ. Pollut. 102, 63–75.
Gigliotti, C.L., Brunciak, P.A., Dachs, J., Glenn, T.R., Nelson, E.D., Totten, L.A., Eisenreich, S.J., 2002. Air-water exchange of polycyclic aromatic hydrocarbons in the New York-New Jersey, USA, Harbor Estuary. Environ. Toxicol. Chem. 21, 235–244.
Guitart, C., Garcia-Flor, N., Bayona, J.M., Albaiges, J., 2007. Occurrence and fate of polycyclic aromatic hydrocarbons in the coastal surface microlayer. Mar. Pollut. Bull. 54, 186–194.
Guo, L.C., Bao, L.J., She, J.W., Zeng, E.Y., 2014. Significance of wet deposition to removal of atmospheric particulate matter and polycyclic aromatic hydrocarbons: a case study in Guangzhou, China. Atmos. Environ. 83, 136–144.
Guo, Z.G., Lin, T., Zhang, G., Zheng, M., Zhang, Z.Y., Hao, Y.C., Fang, M., 2007. The sedimentary fluxes of polycyclic aromatic hydrocarbons in the Yangtze River Estuary coastal sea for the past century. Sci. Total Environ. 386, 33–41.
Guo, Z.G., Lin, T., Zhang, G., Yang, Z.S., Fang, M., 2006. High-resolution depositional records of polycyclic aromatic hydrocarbons in the central continental shelf mud of the East China Sea. Environ. Sci. Technol. 40, 5304–5311.
Guo, Z.G., Sheng, L.F., Feng, J.L., Fang, M., 2003. Seasonal variation of solvent extractable organic compounds in the aerosols in Qingdao, China. Atmos. Environ. 37, 1825–1834.
Gustafson, K.E., Dickhut, R.M., 1997. Gaseous exchange of polycyclic aromatic hydrocarbons across the air-water interface of southern Chesapeake Bay. Environ. Sci. Technol. 31, 1623–1629.
He, J., Balasubramanian, R., 2010. The exchange of SVOCs across the air-sea interface in Singapore's coastal environment. Atmos. Chem. Phys. 10, 1837–1852.
Hsu, S.C., Liu, S.C., Arimoto, R., Liu, T.H., Huang, Y.T., Tsai, F.J., Lin, F.J., Kao, S.J., 2009. Dust deposition to the East China Sea and its biogeochemical implications. Journal of Geophysical Research-Atmospheres 114.
Hu, L.M., Guo, Z.G., Shi, X.F., Qin, Y.W., Lei, K., Zhang, G., 2011. Temporal trends of aliphatic and polyaromatic hydrocarbons in the Bohai Sea, China: evidence from the sedimentary record. Org. Geochem. 42, 1181–1193.
Hui, Y.M., Zheng, M.H., Liu, Z.T., Gao, L.R., 2009. Distribution of polycyclic aromatic hydrocarbons in sediments from Yellow River Estuary and Yangtze River Estuary, China. J. Environ. Sci 21, 1625–1631.
Hung, C.C., Ko, F.C., Gong, G.C., Chen, K.S., Wu, J.M., Chiang, H.L., Peng, S.C., Santschi, P.H., 2014. Increased zooplankton PAH concentrations across hydrographic fronts in the East China Sea. Mar. Pollut. Bull. 83, 248–257.
Kavouras, I.G., Koutrakis, P., Tsapakis, M., Lagoudaki, E., Stephanou, E.G., Von Baer, D., Oyola, P., 2001. Source apportionment of urban particulate aliphatic and polynuclear aromatic hydrocarbons (PAHs) using multivariate methods. Environ. Sci. Technol. 35, 2288–2294.
Kim, J.Y., Lee, J.Y., Choi, S.D., Kim, Y.P., Ghim, Y.S., 2012. Gaseous and particulate polycyclic aromatic hydrocarbons at the Gosan background site in East Asia. Atmos. Environ. 49, 311–319.
Kim, S.K., Chae, D.H., 2016. Seasonal variation in diffusive exchange of polycyclic aromatic hydrocarbons across the air-seawater interface in coastal urban area. Mar. Pollut. Bull. 109, 221–229.
Lang, C., Tao, S., Liu, W.X., Zhang, Y.X., Simonich, S., 2008. Atmospheric transport and outflow of polycyclic aromatic hydrocarbons from China. Environ. Sci. Technol. 42, 5196–5201.
Lee, B.K., Lee, C.B., 2004. Development of an improved dry and wet deposition collector and the atmospheric deposition of PAHs onto Ulsan Bay, Korea. Atmos. Environ. 38, 863–871.
Li, J., Cheng, H.R., Zhang, G., Qi, S.H., Li, X.D., 2009. Polycyclic aromatic hydrocarbon (PAH) deposition to and exchange at the air-water interface of Luhu, an urban lake in Guangzhou, China. Environ. Pollut. 157, 273–279.
Lin, T., Hu, L.M., Guo, Z.G., Qin, Y.W., Yang, Z.S., Zhang, G., Zheng, M., 2011. Sources of polycyclic aromatic hydrocarbons to sediments of the Bohai and Yellow Seas in East Asia. Journal of Geophysical Research-Atmospheres 116.
Lin, T., Hu, L.M., Guo, Z.G., Zhang, G., Yang, Z.S., 2013. Deposition fluxes and fate of polycyclic aromatic hydrocarbons in the Yangtze River estuarine-inner shelf in the East China Sea. Global Biogeochem. Cycles 27, 77–87.
Liu, F.B., Xu, Y., Liu, J.W., Liu, D., Li, J., Zhang, G., Li, X.D., Zou, S.C., Lai, S.C., 2013. Atmospheric deposition of polycyclic aromatic hydrocarbons (PAHs) to a coastal site of Hong Kong, South China. Atmos. Environ. 69, 265–272.
Lohmann, R., Dapsis, M., Morgan, E.J., Dekany, V., Luey, P.J., 2011. Determining Air − Water Exchange, Spatial and Temporal Trends of Freely Dissolved PAHs in an Urban Estuary Using Passive Polyethylene Samplers.
Ma, W.L., Sun, D.Z., Shen, W.G., Yang, M., Qi, H., Liu, L.Y., Shen, J.M., Li, Y.F., 2011. Atmospheric concentrations, sources and gas-particle partitioning of PAHs in Beijing after the 29th Olympic Games. Environ. Pollut. 159, 1794–1801.
Ma, Y.X., Xie, Z.Y., Yang, H.Z., Moller, A., Halsall, C., Cai, M.H., Sturm, R., Ebinghaus, R., 2013. Deposition of polycyclic aromatic hydrocarbons in the North Pacific and the Arctic. J. Geophys. Res. Atmos. 118, 5822–5829.
Mai, B.X., Fu, H.M., Sheng, G.Y., Kang, Y.H., Lin, Z., Zhang, G., Min, Y.S., Zeng, E.Y., 2002. Chlorinated and polycyclic aromatic hydrocarbons in riverine and estuarine sediments from Pearl River Delta, China. Environ. Pollut. 117, 457–474.
Mulder, M.D., Heil, A., Kukucka, P., Klanova, J., Kuta, J., Prokes, R., Sprovieri, F., Lammel, G., 2014. Air-sea exchange and gas-particle partitioning of polycyclic aromatic hydrocarbons in the Mediterranean. Atmos. Chem. Phys. 14, 8905–8915.
Nelson, E.D., McConnell, L.L., Baker, J.E., 1998. Diffusive exchange of gaseous polycyclic aromatic hydrocarbons and polychlorinated biphenyls across the air − water interface of the Chesapeake Bay. Environ. Sci. Technol. 32, 912–919.
Nizzetto, L., Lohmann, R., Gioia, R., Jahnke, A., Temme, C., Dachs, J., Herckes, P., Di Guardo, A., Jones, K.C., 2008. PAHs in air and seawater along a North-South Atlantic transect: trends, processes and possible sources. Environ. Sci. Technol. 42, 1580–1585.
Odabasi, M., Sofuoglu, A., Vardar, N., Tasdemir, Y., Holsen, T.M., 1999. Measurement of dry deposition and air-water exchange of polycyclic aromatic hydrocarbons with the water surface sampler. Environ. Sci. Technol. 33, 426–434.
Olivella, M.À., 2006. Polycyclic aromatic hydrocarbons in rainwater and surface waters of Lake Maggiore, a subalpine lake in Northern Italy. Chemosphere 63, 116–131.
Park, J.S., Wade, T.L., Sweet, S., 2001. Atmospheric distribution of polycyclic aromatic hydrocarbons and deposition to Galveston Bay, Texas, USA. Atmos. Environ. 35, 3241–3249.
Parnis, J.M., Mackay, D., Harner, T., 2015. Temperature dependence of Henry's law constants and K-OA for simple and heteroatom-substituted PAHs by COSMO-RS. Atmos. Environ. 110, 27–35.
Qi, W.X., Muller, B., Pernet-Coudrier, B., Singer, H., Liu, H.J., Qu, J.H., Berg, M., 2014. Organic micropollutants in the Yangtze River: seasonal occurrence and annual loads. Sci. Total Environ. 472, 789–799.
Qin, N., He, W., Kong, X.Z., Liu, W.X., He, Q.S., Yang, B., Ouyang, H.L., Wang, Q.M., Xu, F.L., 2013. Atmospheric partitioning and the air-water exchange of polycyclic aromatic hydrocarbons in a large shallow Chinese lake (Lake Chaohu). Chemosphere 93, 1685–1693.
Reisen, F., Arey, J., 2002. Reactions of hydroxyl radicals and ozone with acenaphthene and acenaphthylene. Environ. Sci. Technol. 36, 4302–4311.
Ren, H.F., Kawagoe, T., Jia, H.J., Endo, H., Kitazawa, A., Goto, S., Hayashi, T., 2010. Continuous surface seawater surveillance on poly aromatic hydrocarbons (PAHs) and mutagenicity of East and South China Seas. Estuar. Coast Shelf Sci. 86, 395–400.
Sahu, S.K., Pandit, G.G., Sadasivan, S., 2004. Precipitation scavenging of polycyclic aromatic hydrocarbons in Mumbai, India. Sci. Total Environ. 318, 245–249.
Schifman, L.A., Boving, T.B., 2015. Spatial and seasonal atmospheric PAH deposition patterns and sources in Rhode Island. Atmos. Environ. 120, 253–261.
Sheu, H.L., Lee, W.J., Hwang, K.P., Liow, M.C., Wu, C.C., Hsieh, L.T., 1996. Dry deposition velocities of polycyclic aromatic hydrocarbons in the ambient air of traffic intersections. J. Environ. Sci. Health Part A Environ. Sci. Eng. Toxic Hazard. Subst. Control 31, 2295–2311.
Tang, N., Hakamata, M., Sato, K., Okada, Y., Yang, X., Tatematsu, M., Toriba, A., Kameda, T., Hayakawa, K., 2015. Atmospheric behaviors of polycyclic aromatic hydrocarbons at a Japanese remote background site, Noto peninsula, from 2004 to 2014. Atmos. Environ. 120, 144–151.
Terzi, E., Samara, C., 2005. Dry deposition of polycyclic aromatic hydrocarbons in urban and rural sites of Western Greece. Atmos. Environ. 39, 6261–6270.
Tobiszewski, M., Namiesnik, J., 2012. PAH diagnostic ratios for the identification of pollution emission sources. Environ. Pollut. 162, 110–119.
Tsapakis, M., Apostolaki, M., Eisenreich, S., Stephanou, E.G., 2006. Atmospheric deposition and marine sedimentation fluxes of polycyclic aromatic hydrocarbons in the eastern Mediterranean basin. Environ. Sci. Technol. 40, 4922–4927.
Vardar, N., Esen, F., Tasdemir, Y., 2008. Seasonal concentrations and partitioning of PAHs in a suburban site of Bursa, Turkey. Environ. Pollut. 155, 298–307.
Wang, F.J., Chen, Y., Meng, X., Fu, J.P., Wang, B., 2016. The contribution of

anthropogenic sources to the aerosols over East China Sea. Atmos. Environ. 127, 22–33.
Wang, F.W., Guo, Z.G., Lin, T., Hu, L.M., Chen, Y.J., Zhu, Y.F., 2015. Characterization of carbonaceous aerosols over the East China Sea: the impact of the East Asian continental outflow. Atmos. Environ. 110, 163–173.
Wang, F.W., Lin, T., Li, Y.Y., Ji, T.Y., Ma, C.L., Guo, Z.G., 2014a. Sources of polycyclic aromatic hydrocarbons in PM2.5 over the East China Sea, a downwind domain of East Asian continental outflow. Atmos. Environ. 92, 484–492.
Wang, J.Z., Guan, Y.F., Ni, H.G., Luo, X.L., Zeng, E.Y., 2007. Polycyclic aromatic hydrocarbons in riverine runoff of the pearl river delta (China): concentrations, fluxes, and fate. Environ. Sci. Technol. 41, 5614–5619.
Wang, X.L., Liu, S.Z., Zhao, J.Y., Zuo, Q., Liu, W.X., Li, B.G., Tao, S., 2014b. Deposition flux of aerosol particles and 15 polycyclic aromatic hydrocarbons in the North China Plain. Environ. Toxicol. Chem. 33, 753–760.
Wu, Z., Lin, T., Li, Z., Jiang, Y., Li, Y., Yao, X., Gao, H., Guo, Z., 2017. Air–sea exchange and gas–particle partitioning of polycyclic aromatic hydrocarbons over the northwestern Pacific Ocean: Role of East Asian continental outflow. Environ. Pollut. 230, 444–452.
Xu, S.S., Liu, W.X., Tao, S., 2006. Emission of polycyclic aromatic hydrocarbons in China. Environ. Sci. Technol. 40, 702–708.
Yang, Y.Y., Guo, P.R., Zhang, Q., Li, D.L., Zhao, L., Mu, D.H., 2010. Seasonal variation, sources and gas/particle partitioning of polycyclic aromatic hydrocarbons in Guangzhou, China. Sci. Total Environ. 408, 2492–2500.
Yunker, M.B., Macdonald, R.W., Vingarzan, R., Mitchell, R.H., Goyette, D., Sylvestre, S., 2002. PAHs in the Fraser River basin: a critical appraisal of PAH ratios as indicators of PAH source and composition. Org. Geochem. 33, 489–515.
Zhang, A.G., Zhao, S.L., Wang, L.L., Yang, X.L., Zhao, Q., Fan, J.F., Yuan, X.T., 2016. Polycyclic aromatic hydrocarbons (PAHs) in seawater and sediments from the northern Liaodong Bay, China. Mar. Pollut. Bull. 113, 592–599.
Zhang, J., Zhang, G.S., Bi, Y.F., Liu, S.M., 2011. Nitrogen species in rainwater and aerosols of the Yellow and East China seas: effects of the East Asian monsoon and anthropogenic emissions and relevance for the NW Pacific Ocean. Global Biogeochem. Cycles 25, 14.
Zhang, K., Gao, H.W., 2007. The characteristics of Asian-dust storms during 2000-2002: from the source to the sea. Atmos. Environ. 41, 9136–9145.
Zhu, Y.H., Yang, L.X., Yuan, Q., Yan, C., Dong, C., Meng, C.P., Sui, X., Yao, L., Yang, F., Lu, Y.L., Wang, W.X., 2014. Airborne particulate polycyclic aromatic hydrocarbon (PAH) pollution in a background site in the North China Plain: concentration, size distribution, toxicity and sources. Sci. Total Environ. 466–467, 357–368.